J. Mech. Phys. Solids Vol. 40, No. 5, pp. 1139–1162, 1992.
Printed in Great Britain.

0022-5096/92 $5.00+0.00

YIELDING OF METAL POWDER BONDED BY ISOLATED CONTACTS

N. A. FLECK

Cambridge University Engineering Department, Trumpington St, Cambridge CB2 1PZ, U.K.

and

L. T. KUHN and R. M. MCMEEKING†

Department of Materials and Department of Mechanical Engineering, University of California, Santa Barbara, CA 93106, U.S.A.

(*Received* 20 *November* 1990)

ABSTRACT

A MACROSCOPIC constitutive law is developed for the plastic yielding of a random aggregate of perfectly plastic spherical metal particles. The particles are bonded perfectly by isolated contacts and deformation occurs by plastic yielding of material at and near these contacts. The configuration is treated as isotropic and homogeneous as far as particle size and properties are concerned. The results are considered valid for aggregates with densities ranging from about 60% to around 90% of the theoretical fully dense level. The yield surface is obtained from the plastic dissipation at necks between particles given an imposed macroscopically uniform strain rate. The contact yield surface resulting from this analysis is sensitive to pressure as well as to deviatoric stress. The plastic strain rate direction is outwardly normal to the yield surface. Densification takes place when pressure is present, but a notable feature is a vertex on the yield surface at the points of pure positive and negative pressure. Consequently, plastic flow in the presence of pure pressure is nonunique, and deviatoric components may be superposed on densification.

1. POWDER CONSOLIDATION

A PRIMARY purpose of this paper is to present a constitutive law for the yielding of powder compacts at low relative densities in the range 0.64–0.9. The yield condition is applicable to the process of powder consolidation by pressing. In such processes, powder particles are packed initially in a can or other container at a random close packing density of around $D_0 = 0.64$ (HELLE *et al.*, 1985). Then the compact is densified by the application of pressure and/or heat in the case of isostatic pressing or by uniaxial stress with or without heating in the case of pressing. In HIPing (hot isostatic pressing), or CIPing (cold isostatic pressing) the macroscopic deformation during consolidation is nominally isotropic. However, nonuniformities of temperature and constraint due to the can may lead to shape changes (LI *et al.*, 1987; WADLEY *et al.*, 1991) so that macroscopic deviatoric straining occurs. Also, uniaxial pressing

† Author to whom correspondence should be addressed.

involves a deviatoric component of deformation. In order that comprehensive predictive models can be assembled, macroscopic constitutive laws accounting for deviatoric straining as well as volume change must be developed. Such constitutive laws could also be used for the consolidation of powders around rigid reinforcements to make composite materials, and for deformation modeling of incompletely pressed products made by powder metallurgy. For example, sintered bronze bushes are used in plain journal bearings. Sintered steel gears and cams find application in the automotive industry. Sintered polymers such as PTFE are used in the base of snow skis. In order to model the mechanics of indentation, wear and fracture in these materials, constitutive laws are required.

Various regimes of deformation for powder aggregates have been identified (HELLE *et al.*, 1985). However, in this paper we will be concerned with situations in which the deformation is controlled by contacts between particles. This is thought to prevail when the relative density D ranges from the random close packed value of 0.64 up to around 0.9 (HELLE *et al.*, 1985). Above that level, the porosity closes off and pore channels or voids then determine the rate at which deformation takes place. Here we address only the plastic yielding case and leave creep, whether power law or diffusion controlled, for later treatment. Furthermore, we are concerned only with a homogeneous spherical powder of uniform size.

Ashby and co-workers (HELLE *et al.*, 1985; ARZT, 1982; ARZT *et al.*, 1983) have developed a macroscopic yield condition for the case where contacts control the deformation, but only for the situation of purely hydrostatic stress. This yield condition is

$$p_y = 2.97D^2\frac{(D-D_o)}{(1-D_o)}\sigma_Y, \tag{1.1}$$

where p_y is the macroscopic pressure to cause yield and σ_Y is the uniaxial yield stress of the metal composing the powder particles. The macroscopic deformation in response to the yielding is assumed to be purely densification without shearing.

An interesting feature of the yield condition (1.1) is that the yield pressure is zero when $D = D_o = 0.64$ because then the particles touch only at points. As the relative density increases towards unity, the yield pressure rises. However, the condition is not meant to apply above $D = 0.9$ so that the finite yield pressure when $D = 1$ is meaningless. The yield condition (1.1) has been used successfully by HELLE *et al.* (1985) and ASHBY (1990) in extensive comparisons with HIPing experiments. Thus, it must be considered to be a reliable criterion. Therefore, any more general yield condition accounting for deviatoric stresses as well as pressure should be made to agree with (1.1) in the limit of hydrostatic loading.

In this paper, we describe a yield model for a random distribution of spherical particles which are joined by necks of finite size. After describing the basic elements of the model, the yield surface is calculated for axisymmetric loading of the aggregate. Simple but approximate expressions are constructed for the yield surface under general loading, and the model is compared with the well-known porous plasticity law of GURSON (1977). A full constitutive prescription is given for the particle model assuming the matrix material is made from elastic–strain hardening plastic material.

This paper ends with an analytical prediction of the uniaxial compression behavior for an aggregate of particles made from rigid–power law hardening material.

2. MODEL FOR THE YIELD SURFACE

Consider a macroscopic element of the powder compact containing many particles as depicted in Fig. 1. It is composed of powder particles of equal size randomly arranged so that the relative density is D, with $0.64 \leqslant D < 0.9$. The particles are perfectly bonded together at isolated contacts. Due to the random arrangement of the particles, the aggregate is macroscopically uniform and isotropic.

For such an isotropic aggregate, HELLE *et al.* (1985) have shown that the number of contacts per particle Z increases in an approximately linear fashion with the relative density D:

$$Z = 12D. \tag{2.1}$$

Thus Z equals around 8 at a dense random packing of $D = D_o = 0.64$ and has a value of 12 at full density. HELLE *et al.* (1985) infer that the average area A_c of one contact is

$$A_c = \frac{\pi}{3}\left(\frac{D-D_o}{1-D_o}\right)R_o^2, \tag{2.2}$$

where R_o is the particle radius (see Fig. 2). Thus the total average area of contact per particle is approximately

$$ZA_c = 4\pi D\left(\frac{D-D_o}{1-D_o}\right)R_o^2. \tag{2.3}$$

A unit cell of radius R and volume V shown in Fig. 2 is defined for each particle so that

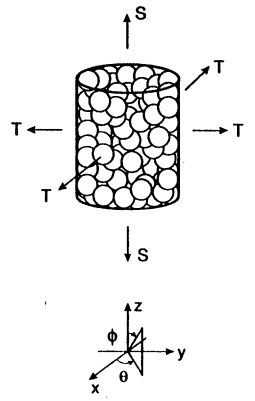

FIG. 1. Macroscopic element of powder aggregate under remote axisymmetric loading.

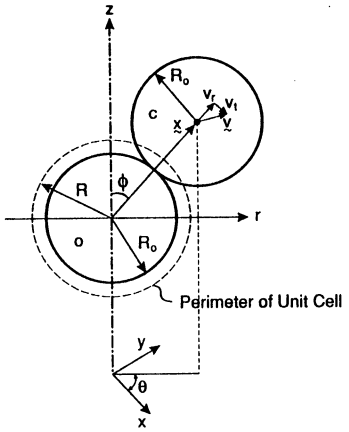

FIG. 2. Typical contact between spherical particles, and definition of coordinate system.

$$V = 4\pi R_o^3/3D. \tag{2.4}$$

Consider a macroscopic virtual isostatic consolidation in which the unit cell volume collapses at the rate $\dot{V}$. The virtual work rate of an applied pressure p_y is $p_y\dot{V}$. During this process the particle centers move towards each other at a speed $2R_o\dot{V}/3V$. By assuming that the compression on each contact is equal to the fully constrained Prandtl punch value of $[(2+\pi)/\sqrt{3}]\sigma_y = 2.97\sigma_y$ (HILL, 1950), HELLE *et al.* (1985) deduced that the plastic dissipation rate per unit area at each contact is $5.94\sigma_y R_o\dot{V}/3V$. Multiplication of this by ZA_c and division by 2 (each contact is shared by two particles) provides the plastic dissipation rate per particle. This must equal the external virtual work rate apportioned to each particle so it can be equated to $p_y\dot{V}$. Equation (2.4) can then be used to establish the result (1.1) given by HELLE *et al.* (1985). This formula can be used with p_y representing either positive or negative pressure. Using a similar method, we will now generalize this result to nonisostatic stress states.

The method of BISHOP and HILL (1951) will be used to estimate the macroscopic yield surface for a random aggregate of rigid–perfectly plastic particles. In this method, a velocity field throughout the body is derived from a uniform macroscopic strain rate $\dot{\mathbf{E}}$. The internal plastic dissipation rate per unit macroscopic volume $\dot{W}^p$ is computed for the assumed velocity field. Then, according to a result introduced by GURSON (1977), the dissipation rate per unit volume is differentiated with respect to the macroscopic strain rate to give the macroscopic stress $\boldsymbol{\Sigma}$ associated with the plastic strain rate $\dot{\mathbf{E}}$. That is

$$\Sigma_{ij} = \partial\dot{W}^p(\dot{\mathbf{E}})/\partial\dot{E}_{ij}. \tag{2.5}$$

This method is equivalent to the original BISHOP and HILL (1951) upper-bound calculation, so that the locus in stress space resulting from (2.5) is an upper bound to the actual yield surface.

Consider a typical contact between neighboring particles as shown in Fig. 2. Due to the assumed field, the velocity of particle C with respect to particle O is $\mathbf{v}$. The component of this velocity in the direction OC moving C away from O is $v_n(\phi,\theta)$; $v_t(\phi,\theta)$ is the velocity component orthogonal to OC, where the angular coordinates ϕ and θ are defined in Fig. 2. Plastic deformation takes place near the contact of the two particles, and average normal and shear tractions $\sigma_{nn}(\phi,\theta)$ and $\sigma_{nt}(\phi,\theta)$ act across the contact area. As a result, the total plastic dissipation rate per unit area of contact is

$$\dot{W}^p_A(\phi,\theta) = \sigma_{nn}v_n + \sigma_{nt}v_t. \tag{2.6}$$

This plastic dissipation occurs over two particles so half of it is apportioned to each particle. Let the probability be $f(\phi,\theta)$ that a contact will be found at (ϕ,θ) so that the average plastic dissipation per particle is

$$\dot{W}^p_p = \frac{1}{2}\int_{S_o} f(\phi,\theta)\dot{W}^p_A(\phi,\theta)\,\mathrm{d}S_o, \tag{2.7}$$

where S_o is the surface area of particle O. To compute the plastic dissipation per unit macroscopic volume this must be multiplied by D/V_p, where V_p is the volume of one particle. Thus

$$\dot{W}^p = \frac{3D}{8\pi R_o^3}\int_{S_o} f(\phi,\theta)\dot{W}^p_A(\phi,\theta)\,\mathrm{d}S_o. \tag{2.8}$$

This result in conjunction with (2.5) can be used to determine the macroscopic stress required to cause yield given an assumed velocity field.

In the isotropic case, the probability f is uniform and equal to the average area of contact on the particle surface ZA_c divided by the particle surface area $S_o = 4\pi R_o^2$. In that case

$$\dot{W}^p = \frac{3D^2(D-D_o)}{8\pi R_o^3(1-D_o)}\int_{S_o}\dot{W}^p_A(\phi,\theta)\,\mathrm{d}S_o$$

$$= \frac{p_y}{8\pi R_o^3\sigma_y}\int_{S_o}(\sigma_{nn}v_n + \sigma_{nt}v_t)\,\mathrm{d}S_o. \tag{2.9}$$

3. AXISYMMETRIC DEFORMATION

We consider the state of macroscopic stress $\boldsymbol{\Sigma}$ shown in Fig. 1, where

$$\Sigma_{zz} = S \quad \text{and} \quad \Sigma_{xx} = \Sigma_{yy} = T. \tag{3.1}$$

The associated macroscopic strain rate is $\dot{\mathbf{E}}$, with components $\dot{E}_{zz}$ and $\dot{E}_{xx} = \dot{E}_{yy}$. The macroscopic dilatation rate is $\dot{H}$ and the distortional rate is $\dot{E}$, where

$$\dot{H} = \dot{E}_{zz} + 2\dot{E}_{xx}, \quad \dot{E} = \tfrac{2}{3}(\dot{E}_{zz} - \dot{E}_{xx}). \tag{3.2}$$

The assumed kinematic field in the particulate aggregate is one in which the centers of the particles move compatibly with the macroscopic homogeneous rate $\dot{\mathbf{E}}$. We place

the center of a typical particle at the origin. The velocity $\mathbf{v}$ of the center of a neighboring particle at $\mathbf{x}$ is assumed to be

$$v_i = \dot{E}_{ij} x_j. \tag{3.3}$$

Note that we have omitted the uniform velocity and the spin rate since they are irrelevant to our model.

Given the strain rates specified in (3.2), the motion of the particle centered at C in Fig. 2 relative to the particle centered at the origin is

$$v_n = R_o[\dot{E}(3\cos^2\phi - 1) + 2\dot{H}/3] \tag{3.4}$$

and

$$v_t = -3R_o\dot{E}\sin\phi\cos\phi. \tag{3.5}$$

For a rigid–perfectly plastic material, plastic deformation occurs in a region adjacent to the neck between particles. We restrict the local deformation field in the neck to plane strain, and thereby calculate the plastic dissipation from the slip line field solution of GREEN (1954). An outline of the slip line field is shown in Fig. 3. The configuration shown arises when $|\alpha| \geqslant \pi/4$. The angle HJK must be α, where

$$\tan\alpha = v_t/v_n = -3\dot{E}\sin\phi\cos\phi/[\dot{E}(3\cos^2\phi - 1) + 2\dot{H}/3] \tag{3.6}$$

to ensure that the material outside the shown slip lines can move rigidly and compatibly with the deforming material. The area $HIJK$ is a region of uniform stress and when $\beta = 0$ has components

$$\left.\begin{aligned} \sigma_{nn} &= k(1 + 3\pi/2 + 2\alpha - \sin 2\alpha) \\ \sigma_{nt} &= k\cos 2\alpha \end{aligned}\right\} -\pi/2 \leqslant \alpha \leqslant -\pi/4, \tag{3.7, 3.8}$$

$$\left.\begin{aligned} \sigma_{nn} &= k(1 + 3\pi/2 - 2\alpha + \sin 2\alpha) \\ \sigma_{nt} &= -k\cos 2\alpha \end{aligned}\right\} \pi/4 \leqslant \alpha \leqslant \pi/2, \tag{3.9, 3.10}$$

where k is the yield stress in shear. If α, computed accordingly to (3.6), has a magnitude

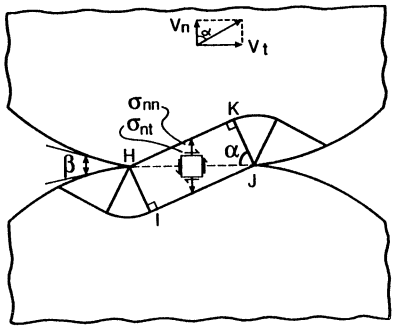

FIG. 3. Slip line field from GREEN (1954) used to calculate the plastic dissipation at each neck between particles.

less than $\pi/4$, then the slip line configuration is simply the Prandtl punch field (HILL, 1950) with the angle HJK equal to $\pi/4$. The stresses are then the Prandtl values

$$\left.\begin{aligned} \sigma_{nn} &= k(2+\pi) \\ \sigma_{nt} &= 0 \end{aligned}\right\} -\pi/4 \leqslant \alpha \leqslant \pi/4. \tag{3.11, 3.12}$$

The assumption that $\beta = 0$ is valid strictly only for an infinitesimal neck. However, these stresses will be taken to apply for any size contact. The locus of stress states possible at the contact during yielding is shown in Fig. 4. As indicated in Fig. 4, the velocities obey a normality rule in association with the yield surface for the neck. At the vertices on the σ_{nn}-axis, the velocity direction can lie anywhere within the sector bounded by the normals to the adjacent segments of the yield surface, i.e. from $-\pi/4$ to $\pi/4$ from the horizontal. This is in accord with the nonuniqueness of the Prandtl punch solution (HILL, 1950). The collapse locus in Fig. 4 shows several noteworthy features. For α in the range $-\pi/4 \leqslant \alpha \leqslant \pi/4$, σ_{nt} vanishes and the contact experiences normal loading with $\sigma_{nn} = k(2+\pi)$. This corresponds to a fixed vertex on the collapse locus (Fig. 4). In the limit where the upper particle shears over the lower particle, a flat exists on the collapse locus and we find $\sigma_{nt} = \pm k$. The normal stress σ_{nn} is indeterminate but lies in the range $-k(1+\pi/2) \leqslant \sigma_{nn} \leqslant k(1+\pi/2)$, and dissipates no energy since $v_n = 0$.

We assume that the average traction at a circular neck between particles is given by the above slip line field solution (3.7)–(3.12). We are unaware of any three-dimensional calculations of the collapse response at a neck in combined tension and shear to validate this assumption. However, SHIELD (1955) has calculated the mean pressure $\bar{p}$ for indentation by a rigid circular cylinder into a half-space made from rigid–perfectly plastic Tresca material. He finds $\bar{p} = 5.69k$, where k is the shear yield stress of the Tresca material. This pressure differs by 10% from the Prandtl punch value, $p = (2+\pi)k$, for plane strain normal indentation by a square punch. This gives us confidence in our two-dimensional model for the plastic dissipation at a neck.

We are concerned with the dissipation at the necks of an isotropic aggregate of particles under axisymmetric straining. Thus the stresses and velocities depend on ϕ but not on θ, and (2.9) becomes

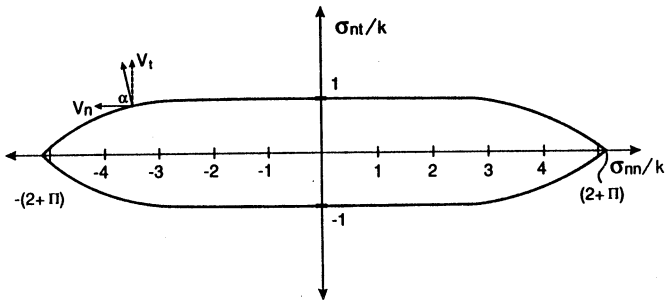

FIG. 4. Yield surface for a contact between two particles [from GREEN (1954)].

$$\dot{W}^p = \frac{p_y}{4R_o\sigma_y}\int_0^{\pi}(\sigma_{nn}v_n + \sigma_{nt}v_t)\sin\phi\,\mathrm{d}\phi, \tag{3.13}$$

with the stresses and velocities given by (3.4)–(3.12). Note that the integrand is proportional to k ($=\sigma_y/\sqrt{3}$ based on a von Mises yield criterion for the powder material which we will use henceforth) and proportional also to R_o. Thus the plastic dissipation rate $\dot{W}^p$ is a function only of $p_y = p_y(D, \sigma_y)$ and of the strain rates $\dot{E}$ and $\dot{H}$. Also, the relative density appears only in the coefficient multiplying the integral in (3.13). Thus, the integral can be computed in a form which is independent of relative density.

4. RESULTS

The integral in (3.13) has been computed for all ratios $\dot{H}/\dot{E}$ and the results are shown in Fig. 5. The dashed line extensions represent the plastic dissipation rate when all contacts around the particles are yielding at the same vertex on the collapse locus in Fig. 4. The function is then linear in $\dot{H}/\dot{E}$ all the way out to $\pm\infty$. The results represented by the full line arise when some (though never all) of the contacts experience a stress state away from the vertices.

We now introduce two new stress measures, Σ_m and Σ. Σ_m is the mean stress defined by

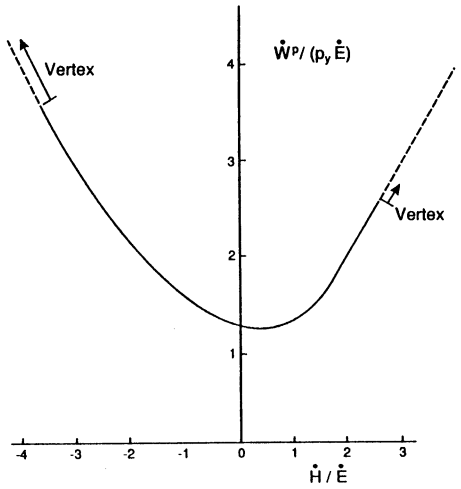

FIG. 5. Plastic dissipation rate ($\dot{W}^p$) as a function of strain rate ratio $\dot{H}/\dot{E}$, where $\dot{H}$ is the dilatation strain rate and $\dot{E}$ is the distortional strain rate.

$$\Sigma_m = \tfrac{1}{3}\Sigma_{kk} = (S+2T)/3 \tag{4.1}$$

and Σ is a measure of the deviatoric stress, given by

$$\Sigma = S - T. \tag{4.2}$$

Note that Σ is closely related to the effective stress $\Sigma_e = (\tfrac{3}{2}\Sigma'_{ij}\Sigma'_{ij})^{1/2}$ by $\Sigma_e = |\Sigma|$, where Σ' is the macroscopic deviatoric stress tensor.

Note that Σ_m and Σ are the work conjugates of $\dot{H}$ and $\dot{E}$, respectively. Following GURSON (1977), values for Σ_m and Σ which lie on the macroscopic yield surface are obtained by differentiation of $\dot{W}^p$ with respect to $\dot{H}$ and $\dot{E}$. Thus

$$\Sigma_m = \frac{\partial \dot{W}^p}{\partial \dot{H}} \tag{4.3}$$

and

$$\Sigma = \partial \dot{W}^p/\partial \dot{E}. \tag{4.4}$$

The calculations were carried out by first differentiating the integrand of (3.13) and then carrying out the integrations numerically. The result is a yield locus of Σ vs Σ_m as shown in Fig. 6 (marked numerical results).

GURSON (1977) has shown that the macroscopic strain rate $\dot{E}_{ij}$ is normal to the yield surface $\phi(\Sigma)$ when the yield surface is calculated using the Bishop–Hill assumption that the microscopic strain rate equals the macroscopic strain rate. Thus the strain rate vector with components $(\dot{H}, \dot{E})$ is normal to the yield surface $\phi(\Sigma_m, \Sigma) = 0$ as shown in Fig. 6.

A vertex exists on the yield surface at $|\Sigma_m| = p_y$, $\Sigma = 0$. This corresponds to radial stressing at particle contacts of all orientations. All necks experience radial stressing

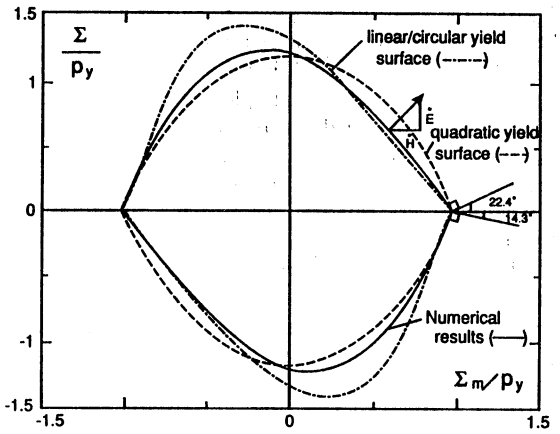

FIG. 6. Yield surface for axisymmetric loading of an isotropic homogeneous aggregate of rigid–perfectly plastic spheres. Accurate numerical values are calculated via (4.3) and (4.4). The approximate linear/circular yield surface is given by (5.3)–(5.6), and the approximate quadratic yield surface is given by (5.17).

when $|\alpha| < \pi/4$, according to (3.7)–(3.12). We deduce from (3.6) that $|\alpha| < \pi/4$ for all ϕ when $\dot{H}/\dot{E} \geqslant \frac{3}{4}(3\sqrt{2}-1)$ or $\dot{H}/\dot{E} \leqslant -\frac{3}{4}(3\sqrt{2}+1)$. Through normality these critical values of $\dot{H}/\dot{E}$ give the angles of the yield locus at the vertex. Thus the normal to the yield locus is at an angle of 22.4° from the horizontal Σ_m-axis in the first and third quadrants and at an angle of 14.3° from the Σ_m-axis in the second and fourth quadrants.

When yielding occurs at the vertex, the plastic flow of the powder aggregate is free to follow any direction within the limiting normals (at 22.4 and −14.3°) of the adjacent smooth segments of the yield surface. It follows that the deformation associated with yielding at the vertex on the positive Σ_m-axis can have a mixture of dilatation and deviatoric response ranging from $\dot{E}/\dot{H} = -0.25$ to $\dot{E}/\dot{H} = 0.41$, including a purely dilatant flow. All those deformations can occur for the same stress state with $\Sigma_m = p_y$ and $\Sigma = 0$. The fundamental reason for this behavior is the vertex on the yield surface of the isolated contact itself (Fig. 4). This vertex allows neighboring particles freedom to move in directions other than directly towards each other while the stress transmitted across the contact is the fully constrained level of the Prandtl field with no shear stress. This endows the macroscopic strain rate with a similar freedom while the macroscopic stress is pure pressure. In the context of soil plasticity, CALLADINE (1971) has also noted that GREEN's (1954) slip line field for a contact would endow the macroscopic aggregate with similar properties, although he does not conclude that the macroscopic behavior would exhibit a yield surface vertex. Indeed, in reality, the vertex may be absent from the macroscopic yield surface for a variety of reasons. The isolated shape of the contact, possibly inducing three-dimensional deformation as opposed to a plane strain behavior, may preclude the vertex. Furthermore, strain hardening may be sufficient to diffuse the localized shearing necessary for the nonunique flow.

We note further from Fig. 6 that the yield locus $\phi(\Sigma_m, \Sigma) = 0$ is not symmetric about the axes $\Sigma_m = 0$ or $\Sigma = 0$. The yield surface is symmetric to reflections through the origin. If the yield surface depended only upon the effective stress $\Sigma_e = |\Sigma|$ and the mean stress Σ_m then the yield surface $\phi(\Sigma_m, \Sigma) = 0$ would be symmetric about the axes $\Sigma_m = 0$ and $\Sigma = 0$. The lack of symmetry indicates that ϕ depends upon the third stress invariant $J_3 = (\Sigma'_{ij}\Sigma'_{jk}\Sigma'_{ki})^{1/3}$ in addition to Σ_m and Σ_e.

Now consider the same numerical results plotted in Fig. 7 as a yield surface for axisymmetric loading in terms of the alternative stress measures S and T. The vertices in the (Σ_m, Σ) plane are replaced by vertices at $S = T = \pm p_y$ on the (T, S) plane. The calculated yield surface on the (T, S) plane can be interpreted in the following approximate manner. In the first quadrant ($T > 0$, $S > 0$) and in the third quadrant ($T < 0$, $S < 0$) the aggregate yields when the principal stress with the largest magnitude approximately attains the value $\pm p_y$.

The plastic strain rates obey a modified normality rule in terms of the yield surface in Fig. 7. The vector with the components $(2\dot{E}_{xx}, \dot{E}_{zz})$ is oriented in the direction normal to the yield surface at the position (T, S), where T and S cause $\dot{E}_{xx}$ and $\dot{E}_{zz}$. In the first and third quadrants, the plastic flow in response to yielding involves straining mostly in the direction of the largest principal stress with little or no straining in the other directions. That is, if S is the stress predominantly causing yielding, the plastic flow in response is almost uniaxial. If T is the predominant cause of the plasticity, the deformation is almost axisymmetric plane strain. The exception is when

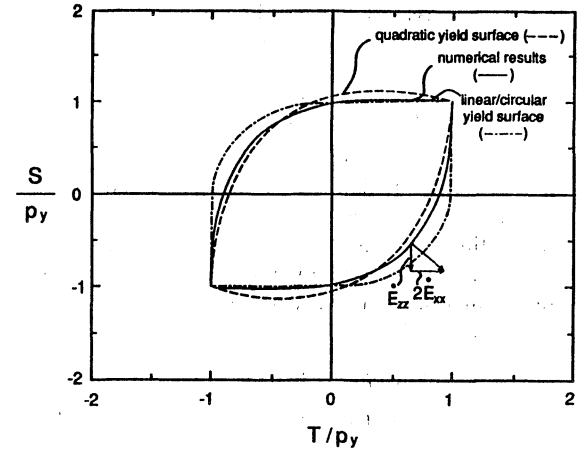

FIG. 7. Yield surface for axisymmetric loading in terms of the radial macroscopic stress T and the axial macroscopic stress S.

yielding occurs at the vertex with $S = T$. Then the plastic flow can range from nearly uniaxial straining through purely hydrostatic deformation to almost plane strain.

Near both the S- and T-axes and in the second and fourth quadrants of stress space in Fig. 7, yielding occurs with some combination of axial and transverse straining. In particular, in a state of uniaxial tension or compression, plastic flow occurs when

$$S = \pm 0.97 p_y \tag{4.5}$$

and

$$\dot{E}_{xx} = \dot{E}_{yy} = -0.11\dot{E}_{zz}. \tag{4.6}$$

Thus, in uniaxial compression, the rate of transverse thickening divided by the current diameter is only 11% of the axial strain rate. It is of interest that in experiments carried out by SHIMA and OYANE (1976) the transverse to axial strain rate ratio in uniaxial compression of copper powder is around −10% when the relative density is around 65%, although it falls to around −40% at higher densities.

5. APPROXIMATE MODELS OF THE YIELD SURFACE

In this section, approximate analytical expressions are derived for the yield surface under axisymmetric loading. We find that the yield surface can be described by a combination of straight lines and circular arcs in the (T, S) plane. Alternatively the yield surface plotted in the (Σ_m, Σ) plane suggests a quadratic fit is adequate.

The yield surface under more general loading is deduced by making additional assumptions. One approach is to assume that the yield surface under general loading depends only on the first two stress invariants, the mean stress Σ_m and the effective

stress Σ_e. Alternatively, we assume that yielding obeys a maximum principal stress criterion.

5.1. *Linear/circular yield surface*

The yield surface in Fig. 7 can be approximated rather well by straight lines in the first and third quadrants and circular arcs in the second and fourth quadrants. This approximation is plotted in Fig. 7 for comparison. The lines used for the approximation in the first and third quadrants are parallel to the axes and are positioned to pass through the result for hydrostatic loading, $|S| = |T| = p_y$. The circular arcs in the second and fourth quadrants are chosen to be continuous with the straight lines and so both arcs are described by

$$(S/p_y)^2 + (T/p_y)^2 = 1. \tag{5.1}$$

The modified normality rule applies, and use of the yield surface approximation predicts that the strain rate direction in the first quadrant is vertical if $S > T$ and horizontal if $T > S$. The vertical direction corresponds to uniaxial strain and the horizontal direction to axisymmetric plane strain. If $S = T = p_y$, the strain rate direction can be anywhere from vertically upwards to rightward horizontal between the limiting normals to the two straight lines. Similar results pertain to the third quadrant. In the second quadrant, the strain rate is such that

$$\dot{E}_{xx} = \dot{E}_{yy} = (T/2S)\dot{E}_{zz} \tag{5.2}$$

for values of S and T agreeing with (5.1). A similar argument is made for the fourth quadrant.

The linear/circular fit can be expressed in terms of the mean stress Σ_m and the deviatoric stress Σ. The result is shown in Fig. 6 and is marked linear/circular yield surface. Extending from the vertices on the pressure axis, the yield surface is composed of straight lines corresponding to the straight lines in the approximate yield surface of Fig. 7. The equations for the straight lines in the linear/circular yield surface when plotted in (Σ_m, Σ) space are:

$$\text{first quadrant:} \quad \phi = 2\Sigma/3p_y + \Sigma_m/p_y - 1 = 0, \tag{5.3}$$

$$\text{second quadrant:} \quad \phi = \Sigma/3p_y - \Sigma_m/p_y - 1 = 0, \tag{5.4}$$

$$\text{third quadrant:} \quad \phi = 2\Sigma/3p_y + \Sigma_m/p_y + 1 = 0, \tag{5.5}$$

$$\text{fourth quadrant:} \quad \phi = \Sigma/3p_y - \Sigma_m/p_y + 1 = 0. \tag{5.6}$$

The strain rate direction in terms of $(\dot{H}, \dot{E})$ is normal to the yield surface in (Σ_m, Σ) space. In conjunction with the straight line segments in the linear/circular yield surface, the strain rates represent uniaxial or axisymmetric plane strain and are such that:

$$\text{first and third quadrants (uniaxial)} \quad \dot{E}/\dot{H} = 2/3, \tag{5.7}$$

$$\text{second and fourth quadrants (plane strain)} \quad \dot{E}/\dot{H} = -1/3. \tag{5.8}$$

At the vertices, the strain rate direction is free to lie anywhere within the normals to the adjacent straight lines. That is, $-1/3 \leqslant \dot{E}/\dot{H} \leqslant 2/3$.

So far, the yield criteria have been developed only for axisymmetric states of stress. We wish to generalize the linear/circular approximation so that the yield criterion and flow law can be used for any three-dimensional state of stress. The generalization will depend on the asumptions made. We use two approaches:

(i) *Assumption: the yield criterion depends only on pressure and the second invariant of deviatoric stress.* This is a common assumption in constitutive modeling of porous metals (DUVA and HUTCHINSON, 1984). Isotropy is assured, and pressure dependence is admitted without the complication of a dependence on all three stress invariants. Since $\Sigma_e = |\Sigma|$, the assumption would be strictly correct if the yield surface were symmetric about both the Σ- and the Σ_m-axis. As was pointed out earlier, this is not true, but the assumption can be pursued in order to obtain a generalized approximation. This is constructed by plotting in (Σ_m, Σ) space the linear/circular approximation contour from the third and fourth quadrants in the first and second quadrants by changing the sign of Σ. The innermost contour is then chosen to represent the yield surface in terms of Σ_m and Σ_e which is then used to represent the criterion for all states of stress. Taking the linear segments only, we find that

$$\phi = 2\Sigma_e/3p_y + \Sigma_m/p_y - 1 = 0 \quad (p_y/3 \leqslant \Sigma_m \leqslant p_y) \tag{5.9}$$

and

$$\phi = 2\Sigma_e/3p_y - \Sigma_m/p_y - 1 = 0 \quad (-p_y \leqslant \Sigma_m \leqslant -p_y/3). \tag{5.10}$$

It should be noted that (5.10) is a specific form of the DRUCKER and PRAGER (1952) yield surface.

The flow law for the powder compact can be developed from the normality rule so that (HILL, 1950)

$$\dot{E}_{ij} = \lambda\, \partial\phi/\partial\Sigma_{ij}, \tag{5.11}$$

where λ is the plastic multiplier. Note that

$$\frac{\partial\Sigma_e}{\partial\Sigma_{ij}} = \frac{3}{2}\frac{\Sigma'_{ij}}{\Sigma_e} \tag{5.12}$$

and

$$\frac{\partial\Sigma_m}{\partial\Sigma_{ij}} = \tfrac{1}{3}\delta_{ij}, \tag{5.13}$$

where δ_{ij} is the Kronecker delta. When contact yield occurs with $p_y/3 \leqslant \Sigma_m < p_y$, the strain rate can be derived from (5.9) and (5.11)–(5.13) as

$$\dot{E}_{ij} = (\lambda/p_y)(\Sigma'_{ij}/\Sigma_e + \tfrac{1}{3}\delta_{ij}). \tag{5.14}$$

Plastic flow at the vertices occurs within the cone of limiting normals.

(ii) *An alternative assumption* that can be used to generate a full yield criterion rests on the observation that in the first quadrant of Fig. 7 contact yielding occurs, approximately, when the larger of S and T reaches the value p_y. When there are three different principal stresses, S, T and R, which are all positive, a natural extension of the observation is to assume that contact yielding occurs when the largest of S, T and

R reaches the value p_y. This assumption is confirmed partly by the fact that a three-dimensional calculation of the yield surface indicates that a vertex of the requisite form exists on the hydrostatic stress axis. In the octant in principal stress space where S, T and R are all tensile or all compressive, the macroscopic yield surface would have the shape of the faces of a cube. In the remaining octants, the yield surface has a complicated three-dimensional shape which smoothly connects circular arcs to cubic segments, so that any projection along a principal axis has a shape like Fig. 7. However, we will concern ourselves only with the octants in which S, T and R are all tensile or all compressive. In that case the macroscopic yield surface is described by

$$\phi = (S^2/p_y^2 - 1)(T^2/p_y^2 - 1)(R^2/p_y^2 - 1) = 0 \tag{5.15}$$

in terms of principal stresses or

$$\phi = \left[-\frac{\Sigma_{ij}\Sigma_{ij}}{p_y^2} + \frac{2\,\mathrm{Det}\,(\boldsymbol{\Sigma})}{p_y^3} + \left(\frac{\Sigma_{kk}}{p_y} + 1\right)^2 + 1 \right] \times \left[\frac{\Sigma_{nn}\Sigma_{mm}}{p_y^2} + \frac{2\,\mathrm{Det}\,(\boldsymbol{\Sigma})}{p_y^3} - \left(\frac{\Sigma_{pp}}{p_y} - 1\right)^2 - 1 \right] = 0. \tag{5.16}$$

In principal stress space, this yield surface is a complete cube which has the desirable configuration in the octants where the stresses are either all tensile or all compressive. In the other octants, the yield surface according to our model lies inside the surface described by (5.15) and (5.16).

The flow law in terms of stress components can be found through use of (5.11) and (5.15) or (5.16) as appropriate. When S, T and R are all tensile or compressive, the direction of plastic straining is coaxial with the principal stress which is at the critical value of $\pm p_y$. Thus uniaxial stress will produce uniaxial straining, with zero transverse straining. If more than one principal stress is at the critical value (i.e. at a vertex of the yield surface) then the plastic flow involves an arbitrary linear combination of strain rates associated with the principal stresses which are at the critical value. This is the usual condition at a vertex in which the plastic strain rate direction lies within the limiting normals of the adjacent yield surface segments. In particular, when the stress is a pure hydrostatic tension, the plastic strain rate components can have any magnitude and orientation as long as the principal values are zero or tensile. The reverse will be true in hydrostatic compression.

5.2. *Quadratic yield surface*

As an alternative to the linear/circular forms, we shall develop a quadratic expression for an approximate yield locus in terms of the effective stress Σ_e and the mean stress Σ_m, based upon the numerical results given in Fig. 6. The approximate locus $\phi(\Sigma_m, \Sigma_e)$ is given the following properties:

(1) At $\Sigma_m = 0$ the isotropic aggregate experiences zero hydrostatic straining ($\dot{H} = 0$). Thus the yield locus in the (Σ_m, Σ_e) plane has a horizontal tangent at $\Sigma_m = 0$. In order to bring the approximate yield locus into agreement with the calculated locus at $\Sigma_m = 0$ we ensure that the approximate locus goes through the point $\Sigma_m = 0$, $\Sigma_e = 1.2p_y$.

(2) The approximate yield locus induces the vertex value $\Sigma_m = p_y$, $\Sigma_e = 0$. We assume the vertex persists for the approximate yield locus. As noted above, the normal to the axisymmetric calculated yield locus is at an angle of 22.4° to the horizontal Σ_m-axis for $\dot{H}/\dot{E} > 0$, and is at angle of 14.3° to the horizontal axis for $\dot{H}/\dot{E} < 0$. We assume arbitrarily that the normal to the approximate quadratic locus bisects these two angles and is at an angle of 18.4° to the horizontal Σ_m-axis.

These properties are sufficient to specify a quadratic approximate yield locus $\phi(\Sigma_m, \Sigma_e)$, given by

$$\phi = \left(\frac{\sqrt{5}\Sigma_m}{3p_y}\right)^2 + \left(\frac{5\Sigma_e}{18p_y} + \frac{2}{3}\right)^2 - 1 = 0. \tag{5.17}$$

This yield surface is plotted for comparison in Figs 6 and 7 (marked quadratic yield surface). Because the quadratic approximation is phrased in terms of Σ_m and Σ_e it is suitable for arbitrary states of stress, so further generalization is unnecessary. The plastic strain rate arising from normality [(5.11)] is

$$\dot{E}_{ij} = (5\lambda/9p_y)[(2\Sigma_m/3p_y)\delta_{ij} + (5\Sigma_e/12p_y + 1)\Sigma'_{ij}/\Sigma_e] \tag{5.18}$$

when yielding is taking place away from the vertex. At the vertex, any combination of deviatoric and dilatational straining can occur as long as $\dot{E}_e/|\dot{H}| \leqslant 1/3$, where $\dot{E}_e = \sqrt{\frac{2}{3}\dot{E}'_{ij}\dot{E}'_{ij}}$.

6. Yield Criterion near Full Density

The yield surfaces developed so far in this paper have been designed for relative densities above D_o up to around 90% full density. It is clear that the criteria are unsuitable near full density since they predict a uniaxial yield stress of around $3\sigma_y$ in that limit. The uniaxial yield stress should be limited to no greater than σ_y and it should be lower when $D < 1$. The contact yield surface is based on the assumption that yielding at each neck occurs without interaction with neighboring necks. However, when the contact area is large enough, as at higher relative densities (2.2), the plastic zones from each particle may meet and interact. This will lead to a general yielding and a loss of constraint not modelled properly in the isolated contact calculation.

An estimate of the effect can be obtained by an upper-bound calculation for a purely deviatoric strain rate as given by (3.2) but with $\dot{H} = 0$ and $\dot{E} > 0$. Let the strain rate pointwise equal the macroscopic strain rate. The plastic dissipation rate is then $D\sigma_y\dot{E}$ and (4.4) provides $\Sigma = \Sigma_e = D\sigma_y$ as an upper bound to the yield stress when $\Sigma_m = 0$. In addition to this effect, the porosity at higher relative densities tends to be closed off into channels and voids rather than present as a three-dimensional network (Arzt *et al.*, 1983). Thus the yield surface at higher relative densities should represent

the effect of voids rather than contacts. A yield surface which does so and also enforces the limitation $\Sigma_e = D\sigma_y$ when $\Sigma_m = 0$ is the GURSON (1977) criterion

$$\phi_G = \left(\frac{\Sigma_e}{D\sigma_y}\right)^2 + \frac{2(1-D)}{D^2}\cosh\left(\frac{3\Sigma_m}{2\sigma_y}\right) - \frac{2(1-D)}{D^2} - 1 = 0. \tag{6.1}$$

The Gurson criterion is compared with the contact yield surface for various relative densities in Fig. 8. The contact yield surface plotted in Fig. 8 is that given by the *numerical* calculations and shown in Fig. 6. It can be seen that the contact yield surface lies entirely inside the Gurson yield surface for D less than about 0.77. Thereafter the Gurson yield surface lies inside the contact yield surface for states of stress with low triaxiality, but the contact yield surface always predicts a lower yield strength in pure hydrostatic stress. It is suggested that above $D = 0.77$ the contact yield surface of choice (numerical, linear/circular or quadratic) should be truncated where it crosses the Gurson yield surface and the latter should be used where it lies inside the contact yield surface.

During consolidation, the topology of the porosity changes from a three-dimensional network at low relative densities to isolated voids at high relative densities. Thus the contact yield surface must be dispensed with completely in favor of the Gurson yield criterion above some transition level of density. This transition should occur in a continuous manner so that there are no jumps in yield stress as the density increases. This can be achieved by interpolation between the contact yield criterion and the Gurson criterion over some transitional range of densities. If ϕ_c is the function of stress representing the contact yield criterion and ϕ_G that for Gursonian yielding then in the transition range $D_1 \leqslant D \leqslant D_2$ yielding is controlled by

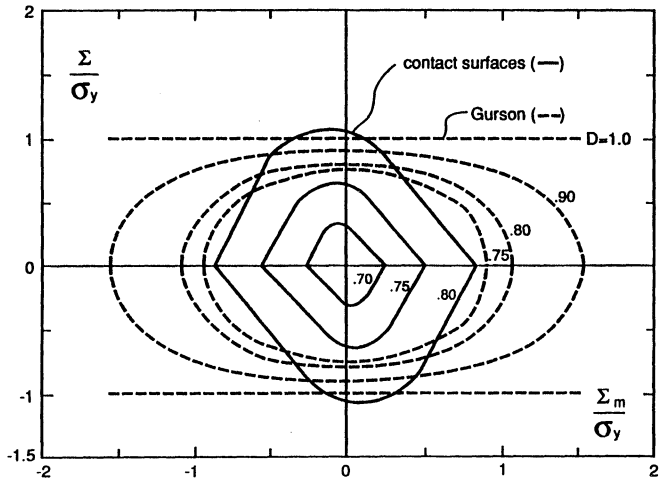

FIG. 8. Contact yield surface (numerical calculations) of Fig. 6 compared with the Gurson criterion (6.1) for various relative densities D.

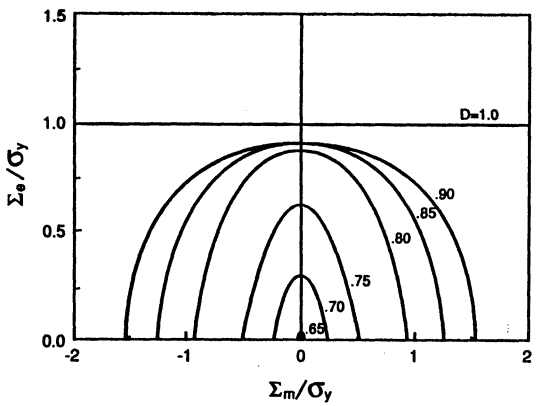

FIG. 9. Suggested family of yield surfaces. For $D < 0.75$, the contact model (quadratic approximation) is used. For $0.75 < D < 0.9$, an interpolation between the contact model and the Gurson model is used. For $D > 0.9$, the Gurson model is used.

$$\phi = \left(\frac{D_2 - D}{D_2 - D_1}\right)\phi_c + \left(\frac{D - D_1}{D_2 - D_1}\right)\phi_G = 0. \tag{6.2}$$

The transition range is a matter of choice. Since $D = 0.77$ is the density level at which interactions between the contact yield zones is clearly evident at low triaxialities, one possibility is to choose $D_1 = 0.75$, invoking contact interaction at high triaxiality at this density too. Perhaps $D_2 = 0.9$ would then be a relevant choice. Another possibility is to use the transition range used by ASHBY (1990) for HIP modelling. He uses $D_1 = 0.8$ and $D_2 = 0.9$ for a transition from contact yielding to a logarithmic criterion exactly equivalent to the GURSON (1977) criterion.

The quadratic yield function offers the simplest framework for handling the complexities of both the truncation of the contact yield surface at low stress triaxialities and the transition to Gurson yielding at high triaxialities. As an illustration, a series of yield loci based on the quadratic approximation have been drawn in Fig. 9 for different relative densities as follows. Below $D = 0.75$, (5.17) serves as the yield surface. The transition to yielding by the Gurson model (6.1) is taken to occur between $D_1 = 0.75$ and $D_2 = 0.9$. Thus, above $D = 0.9$, the yield criterion is that of GURSON (1977).

7. THE CONSTITUTIVE LAW

In order to specify fully the constitutive description for the material, we need to develop rules for the evolution of D and σ_y with continued plastic deformation. Let ϕ be the function of choice representing contact yielding and the transition to the Gurson model. The strain rate arising from the normality rule (5.11) will now be designated the plastic part $\dot{E}^p$ of the total strain rate. Assume the porous aggregate undergoes isotropic hardening or softening during plastic deformation whether due

to geometric effects (density change) or strain hardening. Then the flow law (5.11) can be written as

$$\dot{E}^p_{ij} = \frac{1}{H_m}\frac{\partial \phi}{\partial \Sigma_{ij}}\frac{\partial \phi}{\partial \Sigma_{kl}}\dot{\Sigma}_{kl}, \tag{7.1}$$

where

$$\lambda = \frac{1}{H_m}\frac{\partial \phi}{\partial \Sigma_{kl}}\dot{\Sigma}_{kl} \tag{7.2}$$

has been used based on a standard result (HILL, 1950) in which, following MCMEEKING and RICE (1975), the stress rate has been replaced by the Jaumann rate $\mathring{\boldsymbol{\Sigma}}$ to ensure objectivity to superposed spin. Henceforth $\boldsymbol{\Sigma}$ will be considered to be the macroscopic Cauchy stress. The hardening modulus H_m will depend on the density rate and the strain hardening rate of the material composing the powder.

From conservation of mass,

$$\dot{D} = -D\dot{E}^p_{kk} \tag{7.3}$$

so that

$$\dot{D} = -\frac{D}{H_m}\frac{\partial \phi}{\partial \Sigma_m}\frac{\partial \phi}{\partial \Sigma_{kl}}\dot{\Sigma}_{kl}. \tag{7.4}$$

To account for strain hardening, we take σ_y to represent the average yield stress of deforming material. Thus

$$\Sigma_{ij}\dot{E}^p_{ij} = F(D)\sigma_y\dot{\bar{\varepsilon}}^p, \tag{7.5}$$

where $F(D)$ is the volume fraction of deforming material within the aggregate and $\dot{\bar{\varepsilon}}^p$ is the average effective strain rate in the deforming material. Following GURSON (1977), we assume that σ_y and $\bar{\varepsilon}^p$ are related by the uniaxial tension stress vs plastic-strain curve for the material composing the particles. Thus

$$\dot{\sigma}_y = h(\sigma_y)\dot{\bar{\varepsilon}}^p, \tag{7.6}$$

where $h(\sigma_y)$ is the slope of the graph of the uniaxial Cauchy stress against the plastic part of the logarithmic strain.

The choice for $F(D)$ will depend on the circumstances. For example, GURSON (1977) assumes that all of the solid material in the porous body is deforming plastically and uses $F = D$. This is appropriate for relative density levels above D_2 in which case the yield criterion is that of GURSON (1977). However, when small contacts control yielding, the volume of plastically deforming material is relatively small compared to the particle size. Then F should be less than D. A reasonable approach is to assume that plastic deformation occurs in the particles in hemispherical zones subtended by the circular contacts. Then, from (2.1) and (2.2) we deduce that

$$F(D) = \frac{2}{\sqrt{3}}D^2\left(\frac{D-D_o}{1-D_o}\right)^{3/2}. \tag{7.7}$$

In the transition regime between contact yielding and Gurson yielding it seems sensible to interpolate F as in (6.2).

Finally, we employ the consistency relation for continued plastic flow, $\dot{\phi} = 0$ (HILL, 1950), along with (7.1)–(7.6) to determine H_m. This gives

$$H_m = D\frac{\partial \phi}{\partial D}\frac{\partial \phi}{\partial \Sigma_m} - \frac{h}{F\sigma_y}\frac{\partial \phi}{\partial \sigma_y}\Sigma_{ij}\frac{\partial \phi}{\partial \Sigma_{ij}} \tag{7.8}$$

and (7.5) and (7.6) provide

$$\dot{\sigma}_y = h\frac{\Sigma_{ij}\dfrac{\partial \phi}{\partial \Sigma_{ij}}\dfrac{\partial \phi}{\partial \Sigma_{kl}}\dot{\Sigma}_{kl}}{H_m F\sigma_y}. \tag{7.9}$$

For stress states away from the vertex or for stress increments at the vertex which involve a deviatoric part that therefore moves the stress state away from the vertex, (7.1), (7.4), (7.8) and (7.9) are sufficient to specify the plastic part of the constitutive law. Added to an elastic part

$$\dot{E}^e_{ij} = \frac{1+\nu}{E}\mathring{\Sigma}_{ij} - \frac{\nu}{E}\mathring{\Sigma}_{kk}\delta_{ij}, \tag{7.10}$$

this gives the complete constitutive law for strain rate vs stress rate, where E is a tensile modulus and ν a Poisson's ratio. The elastic moduli should account for Hertzian contact between particles in compression if necessary and thus may be nonlinear in terms of stress (WALTON, 1987). Furthermore E and possibly ν depend on D, an effect which can be modelled using composite theory (CHRISTENSEN, 1979) or based on empirical data (RICE, 1977). Given that

$$\dot{E}_{ij} = \dot{E}^e_{ij} + \dot{E}^p_{ij}, \tag{7.11}$$

the constitutive law can be inverted to give

$$\mathring{\Sigma}_{ij} = \frac{E}{1+\nu}\left\{\dot{E}_{ij} + \frac{\nu}{1-2\nu}\dot{E}_{kk}\delta_{ij} - \frac{1}{\bar{H}}N_{ij}N_{kl}\dot{E}_{kl}\right\}, \tag{7.12}$$

where

$$N_{ij} = \frac{\partial \phi}{\partial \Sigma_{ij}} + \frac{\nu}{1-2\nu}\frac{\partial \phi}{\partial \Sigma_m}\delta_{ij} \tag{7.13}$$

and

$$\bar{H} = \frac{H_m(1+\nu)}{E} + \frac{\partial \phi}{\partial \Sigma_{ij}}\frac{\partial \phi}{\partial \Sigma_{ij}} + \frac{\nu}{1-2\nu}\left(\frac{\partial \phi}{\partial \Sigma_m}\right)^2. \tag{7.14}$$

7.1. *Continued yielding at the vertex*

If continued plastic strain occurs at the vertex in such a way that the stress remains purely hydrostatic then the constitutive law adopts a degenerate form. Subject to the

restriction that the strain rate direction must lie within the limiting normals, the deviatoric part of the strain rate is constitutively indeterminate and must be evaluated from the kinematics of the boundary value problem. Consistency with the yield condition and other considerations require that

$$\dot{E}^p_{kk} = \frac{\partial\phi/\partial\Sigma_m}{D\,\partial\phi/\partial D - [h\Sigma_m(\partial\phi/\partial\sigma_y)/(F\sigma_y)]}\,\dot{\Sigma}_m, \tag{7.15}$$

$$\dot{\sigma}_y = \frac{h\Sigma_m}{F\sigma_y}\,\dot{E}^p_{kk} \tag{7.16}$$

and $\dot{D}$ is given by (7.3) and (7.15). Inversion of (7.15) plus the elastic part gives

$$\dot{\Sigma}_m = \frac{\dot{E}_{kk}}{\dfrac{3(1-2\nu)}{E} + \dfrac{\partial\phi/\partial\Sigma_m}{D\,\partial\phi/\partial D - [h\Sigma_m(\partial\phi/\partial\sigma_y)/(F\sigma_y)]}} \tag{7.17}$$

and the condition that the stress stays purely hydrostatic requires that the deviatoric part of the elastic strain rate is zero.

Specific forms of (7.1)–(7.17) are given in the Appendix for the linear and quadratic approximate yield criteria.

8. UNIAXIAL COMPRESSION

It is instructive to consider the problem of uniaxial compression of an aggregate of particles experiencing plastic flow by yielding at contacts. According to (4.5) the true stress in compression is

$$\sigma = -0.97p_y \tag{8.1}$$

and (4.6) shows that the ratio of transverse plastic strain rate $\dot{\varepsilon}^p_t$ to axial plastic strain rate $\dot{\varepsilon}^p$ is -0.11. Taking $\dot{\varepsilon}^p$ to be negative in compression, we find from (7.3) that

$$\dot{D} = -0.78D\dot{\varepsilon}^p, \tag{8.2}$$

which integrates to give

$$D = D_i e^{-0.78\varepsilon^p}, \tag{8.3}$$

where D_i is the initial density in the compression test. Equations (7.5), (8.1) and (8.2) provide

$$\dot{\bar{\varepsilon}}^p = 1.24\,\frac{p_y\dot{D}}{\sigma_y DF}. \tag{8.4}$$

At this stage, any preferred choice for $F(D)$ can be used, but we proceed with (7.7) so that, given (1.1), integration of (8.4) gives

$$\bar{\varepsilon}^p = 6.39\left(\frac{1-D_o}{D_o}\right)^{1/2}\left[\tan^{-1}\left(\frac{D-D_o}{D_o}\right)^{1/2} - \tan^{-1}\left(\frac{D_i-D_o}{D_o}\right)^{1/2}\right]. \tag{8.5}$$

Any relevant stress–strain curve can be invoked but we choose to use a power law form with

$$\sigma_y = \sigma_o(\bar{\varepsilon}^p/\varepsilon_o)^N. \tag{8.6}$$

We may deduce the true stress vs true (logarithmic) plastic strain curve for the aggregate via (1.1), (8.3), (8.5) and (8.6). In the case where $D_i = D_o$ we find that

$$\sigma = -2.88(6.39)^N\frac{\sigma_o}{\varepsilon_o^N}D_o^{3-N/2}(1-D_o)^{N/2-1}e^{-1.56\varepsilon^p}(e^{-0.78\varepsilon^p}-1)\,[\tan^{-1}(e^{-0.78\varepsilon^p}-1)^{1/2}]^N. \tag{8.7}$$

Plots of $-\sigma\varepsilon_o^N/\sigma_o$ vs ε^p are shown in Fig. 10 for $D_i = D_o = 0.64$ and $N = 0$, 0.1 and 0.2. As shown in Fig. 10, the plot also serves to indicate stress vs relative density D.

ACKNOWLEDGEMENT

This work was supported by the National Science Foundation through Grant DMR-87-13919 to the University of California, Santa Barbara. The authors are grateful for helpful discussions with Professors A. Needleman and M. F. Ashby.

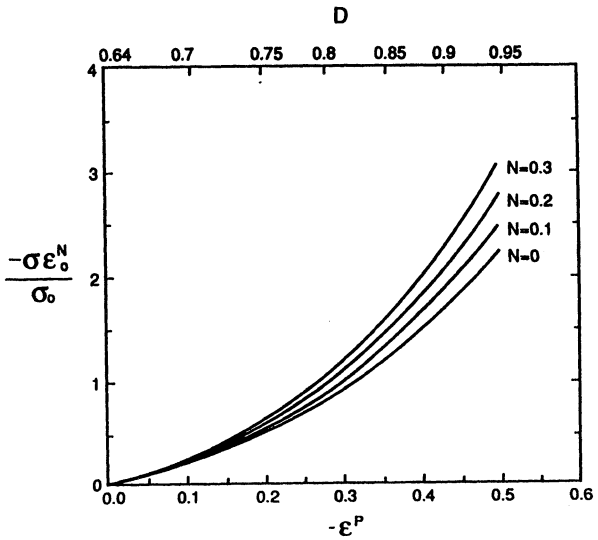

FIG. 10. Macroscopic response of an aggregate of particles made from rigid–strain hardening material. The initial density $D_i = D_o = 0.64$ and N is the strain hardening index.

REFERENCES

ARZT, E. 1982 *Acta metall.* **30,** 1883.
ARZT, E., ASHBY M. F. and EASTERLING, K. E. 1983 *Metall. Trans.* **14A,** 211.
ASHBY, M. F. 1990 *HIP* 6.0, *Background Reading*, Engineering Department, Trumpington St, Cambridge CB2 1PZ, U.K.
BISHOP, J. F. W. and HILL, R. 1951 *Phil. Mag.* **42,** 414, 1298.
CALLADINE, C. R. 1971 *Geotechnique* **21,** 391.
CHRISTENSEN, R. 1979 *Mechanics of Composite Materials.* Wiley, New York.
DRUCKER, D. C. and PRAGER, W. 1952 *Q. appl. Math.* **10,** 157.
DUVA, J. M. and HUTCHINSON, J. W. 1984 *Mech. Mater.* **3,** 41.
GREEN, A. P. 1954 *J. Mech. Phys. Solids* **2,** 197.
GURSON, A. L. 1977 *Trans. ASME Ser. H, J. Engng Mater. Technol.* **99,** 2.
HELLE, A. S., EASTERLING, K. E. and ASHBY, M. F. 1985 *Acta metall.* **33,** 2163.
HILL, R. 1950 *The Mathematical Theory of Plasticity.* Oxford University Press, Oxford.
LI, W.-B., ASHBY, M. F. and EASTERLING, K. E. 1987 *Acta metall.* **35,** 2831.
MCMEEKING, R. M. and RICE, J. R. 1975 *Int. J. Solids Struct.* **11,** 601.
RICE, R. W. 1977 In *Treatise on Materials Science and Technology* (edited by R. K. MACCRONE), Vol. 11, p. 225, Table III. Academic Press, New York.
SHIELD, R. T. 1955 *Proc. R. Soc.* **A233,** 267.
SHIMA, S. and OYANE, M. 1976 *Int. J. Mech. Sci.* **18,** 285.
WADLEY, H. N. G., SCHAEFER, R. J., KAHN A. H., ASHBY, M. F., CLOUGH, R. B., GEFFEN, Y. and WLASSICH, J. J. 1991 *Acta metall. mater.* **39,** 979.
WALTON, K. 1987 *J. Mech. Phys. Solids* **35,** 213.

APPENDIX: CONSTITUTIVE LAW DETAILS

Only the constitutive law for contact yielding is detailed in this Appendix. The transitional form to account for the switch to Gurson yielding is not included. Details will be given in terms of the linear and the quadratic approximate yield functions.

Continued yielding under pure hydrostatic stress

In this case, it does not matter which approximate form is used since both have a vertex on the hydrostatic stress axis at $\Sigma_m = p_y$. Then (7.15) becomes

$$\dot{E}^p_{kk} = \frac{\dot{\Sigma}_m}{\left(\frac{p_y}{\sigma_y}\right)^2 \frac{h}{F} - D\frac{\partial p_y}{\partial D}} \tag{A1}$$

and the deviatoric part of $\dot{\mathbf{E}}^p$ is arbitrary within the limiting normals at the vertex. The elastic–plastic law (7.17) becomes

$$\dot{\Sigma}_m = \frac{\dot{E}_{kk}}{\frac{3(1-2\nu)}{E} + \left[\left(\frac{p_y}{\sigma_y}\right)^2 \frac{h}{F} - D\frac{\partial p_y}{\partial D}\right]^{-1}}. \tag{A2}$$

Linear approximation

Details will be given for the linear portion of the yield surface only. A general form for (5.9) and (5.10) is used such that

$$\phi = A\Sigma_e/p_y + B\Sigma_m/p_y - 1 = 0 \tag{A3}$$

where $A = \frac{3}{2}$, and $B = \Sigma_m/|\Sigma_m|$.

In that case

$$H_m = \frac{h}{F\sigma_y^2} - D\frac{B}{p_y^2}\frac{\partial p_y}{\partial D} \tag{A4}$$

and

$$\dot{E}^p_{ij} = \frac{1}{H_m}\left(\frac{3A\Sigma'_{ij}}{2\Sigma_e p_y} + \frac{B\delta_{ij}}{3p_y}\right)\left(\frac{3A\Sigma'_{kl}\dot{\Sigma}_{kl}}{2\Sigma_e p_y} + \frac{B\dot{\Sigma}_m}{p_y}\right). \tag{A5}$$

The hardening rate is

$$\dot{\sigma}_y = \frac{h}{H_m F\sigma_y}\left(\frac{3A\Sigma'_{kl}\dot{\Sigma}_{kl}}{2\Sigma_e p_y} + \frac{B\dot{\Sigma}_m}{p_y}\right) \tag{A6}$$

and the dilatation rate is

$$\dot{D} = -D\frac{B}{H_m p_y}\left(\frac{3A\Sigma'_{kl}\dot{\Sigma}_{kl}}{2\Sigma_e p_y} + \frac{B\dot{\Sigma}_m}{p_y}\right). \tag{A7}$$

For the inverted form (7.12),

$$N_{ij} = \frac{3A\Sigma'_{ij}}{2\Sigma_e p_y} + \frac{B(1+\nu)\delta_{ij}}{3(1-2\nu)p_y} \tag{A8}$$

and

$$\bar{H} = \frac{H_m(1+\nu)}{E} + \left[\frac{3}{2}A^2 + \frac{(1+\nu)}{3(1-2\nu)}B^2\right]\Big/ p_y^2. \tag{A9}$$

Quadratic approximation

Consider the quadratic yield surface specified by (5.17). The quantities H_m, $\dot{E}^p_{ij}$, $\dot{\sigma}_y$, $\dot{D}$, N_{ij} and $\bar{H}$ are given by (7.8), (7.1), (7.9), (7.13) and (7.14), respectively. Explicit expressions are omitted here since they are lengthy; they may be obtained by substitution for the following derivatives of ϕ:

$$\frac{\partial \phi}{\partial D} = -2\frac{\partial p_y}{\partial D}\left[\frac{5\Sigma_m^2}{9p_y^3} + \frac{5}{18}\frac{\Sigma_e}{p_y^2}\left(\frac{5}{18}\frac{\Sigma_e}{p_y} + \frac{2}{3}\right)\right] \tag{A10}$$

$$= -\frac{10}{9p_y}\frac{\partial p_y}{\partial D}\left(1 - \frac{1}{3}\frac{\Sigma_e}{p_y}\right), \tag{A11}$$

$$\frac{\partial \phi}{\partial \Sigma_m} = \frac{10}{9}\frac{\Sigma_m}{p_y^2}, \tag{A12}$$

$$\frac{\partial \phi}{\partial \sigma_y} = \frac{p_y\, \partial\phi/\partial D}{\sigma_y\, \partial p_y/\partial D}, \tag{A13}$$

$$\frac{\partial \phi}{\partial \Sigma_{ij}} = \frac{5}{6}\left(\frac{5}{18}\frac{\Sigma_e}{p_y} + \frac{2}{3}\right)\frac{\Sigma'_{ij}}{p_y \Sigma_e} + \frac{10}{27}\frac{\Sigma_m}{p_y^2}\delta_{ij} \tag{A14}$$

$$\Sigma_{ij}\frac{\partial \phi}{\partial \Sigma_{ij}} = -\frac{p_y\, \partial\phi/\partial D}{\partial p_y/\partial D}. \tag{A15}$$